

Compressive Slice Encoding for Metal Artifact Correction

W. Lu¹, K. B. Pauly², G. E. Gold², J. M. Pauly³, and B. A. Hargreaves²

¹Electrical & Electronic Engr., Nanyang Tech. University, Singapore, Singapore, ²Radiology, Stanford University, Stanford, CA, United States, ³Electrical Engr., Stanford University, Stanford, CA, United States

Introduction: Slice encoding for metal artifact correction (SEMAC) [1] completely corrects metal-induced in-plane and through-plane distortions. The SEMAC imaging sequence (Fig. 1) augments a view-angle-tilting (VAT) [2] spin echo sequence with z-phase encoding. While the VAT-compensation gradient suppresses the in-plane distortions, the through-plane distortions are corrected by combining multiple 3D slabs, whose distorted excitation profiles are resolved with the z-phase encoding. However, the additional z-phase encoding leads to longer scan times. To accelerate SEMAC acquisition, the SEMAC imaging sequence has been integrated with parallel imaging and partial Fourier acquisition along the y phase encoding direction [3], which nonetheless involves a tradeoff of signal-to-noise ratio (SNR). In this work SEMAC is incorporated with compressed sensing (CS) [4] to reduce both y and z phase encoding. We demonstrate that the new technique, referred to as Compressive SEMAC, can greatly reduce scan times, while producing high-quality distortion correction and SNR comparable to SEMAC with full sampling.

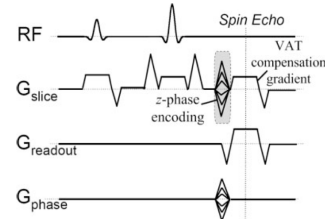


Fig. 1: SEMAC imaging sequence augments a VAT spin echo sequence with z phase encoding.

Methods and Results:

Compressive SEMAC randomly skips both y and z phase encoding steps with a variable-density sampling pattern in $k_y - k_z$ space. The excitation profile in a 3D slab is recovered by performing the following constrained reconstruction at each x location:

$$\begin{aligned} \min \|m_{yz}\|_1 + \lambda \text{TV}(m_{yz}) \\ \text{subject to } \|F_u m_{yz} - Y\| < \varepsilon \end{aligned} \quad (1)$$

where m_{yz} is the optimization

variable corresponding to the distorted excitation profile and $\text{TV}()$ penalizes its total variation with λ empirically set to 1 [4]. The constraint reinforces the data consistency between the under-sampled Fourier transform (F_u) of m_{yz} and the acquired k-space samples Y . The constrained reconstruction is repeated for all slabs to recover their distorted excitation profiles, which are then added to correct the through-plane distortions as in standard SEMAC post-processing procedure [1]. We imaged the knee of a subject who has several stainless steel screws in his tibia at 1.5 T using an 8-channel extremity coil. The variable density under-sampling in $k_y - k_z$ space follows a Poisson random sampling disk suggested in [4], which reduces 65% y and z phase encoding. The scan parameters were: TE/TR=11/540 ms, 32 slices with 3 mm thickness, 256x128 matrix over 16 cm FOV. Figure 2 shows the comparison between spin-echo, SEMAC with full sampling, and compressive SEMAC. Compressive SEMAC demonstrates almost identical correction performance as SEMAC with full sampling in terms of correcting the metal artifacts present in the spin-echo result.

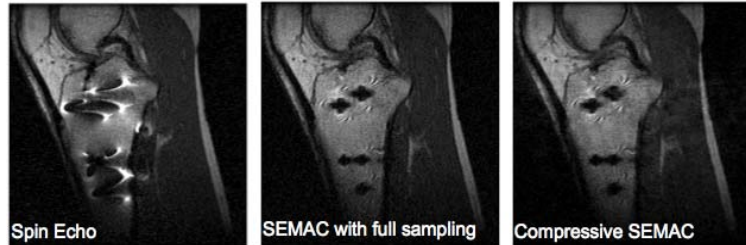


Fig. 2: Comparison of a knee study obtained using spin echo, SEMAC with full sampling, and compressive SEMAC. Compressive SEMAC demonstrates almost identical correction as SEMAC without SNR degradation, given 60% reduction in y and z phase encoding of SEMAC imaging sequence.

where m_{yz} is the optimization variable corresponding to the distorted excitation profile and $\text{TV}()$ penalizes its total variation with λ empirically set to 1 [4]. The constraint reinforces the data consistency between the under-sampled Fourier transform (F_u) of m_{yz} and the acquired k-space samples Y . The constrained reconstruction is repeated for all slabs to recover their distorted excitation profiles, which are then added to correct the through-plane distortions as in standard SEMAC post-processing procedure [1]. We imaged the knee of a subject who has several stainless steel screws in his tibia at 1.5 T using an 8-channel extremity coil. The variable density under-sampling in $k_y - k_z$ space follows a Poisson random sampling disk suggested in [4], which reduces 65% y and z phase encoding. The scan parameters were: TE/TR=11/540 ms, 32 slices with 3 mm thickness, 256x128 matrix over 16 cm FOV. Figure 2 shows the comparison between spin-echo, SEMAC with full sampling, and compressive SEMAC. Compressive SEMAC demonstrates almost identical correction performance as SEMAC with full sampling in terms of correcting the metal artifacts present in the spin-echo result.

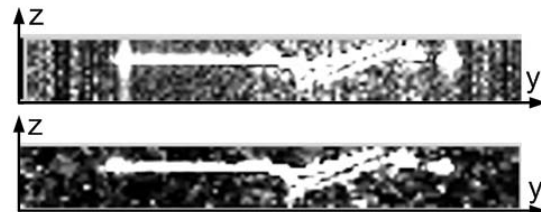


Fig. 3: Sample distorted excitation profiles obtained from (top) SEMAC with full sampling and (bottom) Compressive SEMAC. Note that Compressive SEMAC recovers the sparse excitation profile, and implicitly performs denoising.

Discussion: It is advantageous to incorporate compressed sensing with SEMAC for two main reasons. First, the excitation profiles in the 3D slabs encoded by SEMAC sequences are sparse (Fig. 3: top); hence, no elaborate sparsifying transform is necessary in the CS reconstruction. Second, when recovering the sparse excitation profiles, CS implicitly performs signal denoising, which sets many resolved data containing only background noise to zero (Fig. 3: bottom). Therefore, the reconstruction of SEMAC data using CS inherently excludes background noise in the correction of through-plane distortions. This mitigates the SNR degradation generally associated with under-sampling. MAVRIC [5] is another imaging technique that fully corrects metal artifacts by resolving the sparse profiles in multiple frequency bands; the CS formulation in Eq.1 can also be incorporated with MAVRIC for acceleration. In summary, compressive SEMAC greatly reduces the number of phase encoding steps incurred to resolve metal artifacts, while preserving the distortion correction and the resultant SNR in the corrected images.

References:

- [1] Lu W. et al MRM, 2009; 62(1):66-76. [2] Cho ZH. et al Med. Phys. 1998; 15:7-11. [3] Hargreaves BA. et al ISMRM 2009; p 258. [4] Lustig M. et al MRM, 2007; 58(6): 1182-95. [5] Koch KM. MRM. 2009; 61(2):381-90.

Supported by: NIH-R21EB008190 and AcRF Tier-1 RG25/08